JOURNAL OF GUIDANCE, CONTROL, AND DYNAMICS
Vol. 30, No. 5, September–October 2007

Engineer Notes

ENGINEERING NOTES are short manuscripts describing new developments or important results of a preliminary nature. These Notes should not exceed 2500 words (where a figure or table counts as 200 words). Following informal review by the Editors, they may be published within a few months of the date of receipt. Style requirements are the same as for regular contributions (see inside back cover).

Artificial Equilibrium Points in the Low-Thrust Restricted Three-Body Problem

Mutsuko Y. Morimoto*
Japan Aerospace Exploration Agency, Sagamihara, 229-8510, Japan
Hiroshi Yamakawa†
Kyoto University, Kyoto, 611-0011, Japan
and
Kuninori Uesugi‡
Japan Aerospace Exploration Agency, Kanagawa, 229-8510, Japan

DOI: 10.2514/1.26771

I. Introduction

THE present Note describes the concept of the artificial equilibrium point (AEP) assisted by continuous thrust in the restricted three-body problem (RTBP). In the RTBP, there are five libration points called *Lagrange points*. Each of the Lagrange points is in equilibrium between the gravitational forces of the two primary bodies and the centrifugal force in the rotating frame. The Lagrange points have been investigated in a number of studies in the field of celestial mechanics. Since the 1950s, space engineers have been interested in these Lagrange points and have investigated the applicability of these points to space missions. Farquhar [1] introduced the concept of telecommunication systems using Lagrange points in the Earth–moon system, and in subsequent studies, he investigated ballistic periodic orbits about equilibrium points not only in the Earth–moon system [2–5], but also in the sun–Earth system [6,7].

Currently, low-thrust propulsion systems such as electric propulsion and the solar sail are being developed not only for controlling satellite orbits, but also as main engines for interplanetary transfer. These low-thrust propulsion systems are able to provide continuous control acceleration to the spacecraft and thus to increase mission design flexibility.

When we attempt to use Lagrange points, the positions are normally restricted to only five points. In terms of mission design, however, Lagrange points are not always the best positions. For example, we must operate the satellite at midnight every day when a spacecraft is placed at L2 points, unless we can use a deep space network. L4 and L5 are stable points, but these points are far from the Earth. Therefore, the transfer time required to reach L4/L5 and to telecommunicate is longer than that for points closer to the Earth. To achieve various mission objectives, positions other than the Lagrange points might be suitable in some cases. These points are in nonequilibrium, but it is possible to keep the spacecraft at these positions by using continuous thrust.

Libration points with continuous control acceleration have also been studied (Duseck [8], Simmons et al. [9], McInnes et al. [10,11], and Broschart and Sheeres [12]). In [11], McInnes investigated the magnitude of control acceleration and stability for a two-body problem. These studies reported specific libration points with a certain mass ratio or those with certain low-thrust accelerations. However, for more flexible and generic mission designs, we must analyze arbitral points for the general mass-ratio range with continuous control acceleration by an idealized continuous thrust.

In a previous paper [13], we focused on resonant periodic orbits existing on the line connecting two primary bodies with a continuous-low-thrust propulsion system. On the other hand, in the present Note, we investigate the magnitude and direction of the required acceleration creating the AEP in three-dimensional space. In addition, we discuss its stability by linearizing the equations of motion and carrying out a linear stability analysis.

II. Characteristics of Acceleration for Artificial Equilibrium Points

As shown in [10,13], a nonequilibrium point can be turned into an AEP by applying the appropriate continuous control acceleration $[\boldsymbol{a}_0 = \nabla U(\boldsymbol{r}_0)]$, where $\boldsymbol{a}_0$ is the control acceleration, $\boldsymbol{r}_0 = (x_0, y_0, z_0)$ is the position vector of the AEP from origin to the spacecraft, and U is the sum of the gravitational and centrifugal potentials. In the present Note, all parameters are nondimensional. Thus, the required acceleration components (a_x, a_y, a_z) of $\boldsymbol{a}_0$ in the rotating frame (x, y, z) for the AEP are expressed as

$$a_x = -x_0 + \frac{\mu_1}{r_1^3}(x_0 + \mu_2) + \frac{\mu_2}{r_2^3}(x_0 - \mu_1) \tag{1a}$$

$$a_y = -y_0 + \frac{\mu_1}{r_1^3} y_0 + \frac{\mu_2}{r_2^3} y_0 \tag{1b}$$

$$a_z = \frac{\mu_1}{r_1^3} z_0 + \frac{\mu_2}{r_2^3} z_0 \tag{1c}$$

where r_1 and r_2 are two separate distances between the spacecraft and two primary bodies when $\mu_1 = 1 - \mu$ and $\mu_2 = \mu$ $(\mu_1 > \mu_2)$, both of which are the gravitational constants of the two primaries (see Fig. 1). When $y_0 = 0$, a_y becomes zero, and when $z_0 = 0$, a_z becomes zero. When $x_0 = 0$, a_x becomes as follows:

$$a_x = \frac{\mu_1}{r_1^3}\mu_2 - \frac{\mu_2}{r_2^3}\mu_1 = \mu_1\mu_2\left(\frac{1}{r_1^3} - \frac{1}{r_2^3}\right) \tag{2}$$

From $\mu_1 > \mu_2$, we have $r_1 > r_2$ at $(x_0, y_0, z_0) = (0, 0, 0)$, so that a_x is always positive when $x = 0$.

From Eqs. (1a–1c), we can obtain the direction and magnitude of the acceleration at the AEP. Figure 2 shows plots of $a_x = 0$ and $a_y = 0$ in the X–Y plane, which is the boundary between positive and negative accelerations in the x and y directions.

Received 25 July 2006; revision received 1 May 2007; accepted for publication 17 May 2007.

*Postdoctoral Fellow, 3-1-1 Yoshinodai.
†Professor, Research Institute for Sustainable Humanosphere. Senior Member AIAA.
‡Professor, Institute of Space and Astronautical Science.

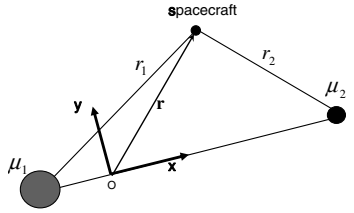

Fig. 1 Rotating frame and relationship between two primary bodies and a spacecraft.

The mass ratio in these figures is assumed to be $\mu = 0.2$. Figure 3 shows the superposition of the two boundaries ($a_x = 0$ and $a_y = 0$) shown in Fig. 2. Because a_z is always zero in this plane, intersections of $a_x = 0$ and $a_y = 0$ in Fig. 3 show five Lagrange points and two primary bodies (M_1 and M_2).

Figure 4 shows the superposition of two boundaries ($a_x = 0$ and $a_y = 0$) for the mass ratio with $\mu = 3.0404 \times 10^{-6}$, corresponding to the sun–Earth system. In the case of a very small mass ratio, such as that of the sun–Earth system, the two boundaries are similar in a macroscopic view (i.e., Fig. 4a), such that the circular region, the center of which is M_1 (e.g., the sun) and the radius of which is the distance between M_1 and M_2 (e.g., the Earth), and these boundaries appear to coincide with each other. In other words, when the mass ratio is very small, the required acceleration is nearly zero in this region in which three Lagrange points (L3, L4, and L5) exist.

III. Stability

In this section, the stability of the AEP is discussed by linearizing the equations of motion and carrying out a linear stability analysis. This corresponds to the behavior of a spacecraft given a small displacement from an AEP.

A. Linearized Equations of Motion

Using $\mathbf{r} = \mathbf{r}_0 + \delta$ [$(\delta = (\delta_x, \delta_y, \delta_z)$], the linearized equations of motion are obtained as (see [13])

$$\frac{\mathrm{d}^2}{\mathrm{d}t^2}\begin{bmatrix}\delta_x\\ \delta_y\\ \delta_z\end{bmatrix} + \frac{\mathrm{d}}{\mathrm{d}t}\begin{bmatrix}-2\delta_y\\ 2\delta_x\\ 0\end{bmatrix} + \begin{bmatrix}U_{xx} & U_{xy} & U_{xz}\\ U_{yx} & U_{yy} & U_{yz}\\ U_{zx} & U_{zy} & U_{zz}\end{bmatrix}\begin{bmatrix}\delta_x\\ \delta_y\\ \delta_z\end{bmatrix} = \mathbf{0} \quad (3)$$

where

$$\left[\frac{\partial}{\partial \mathbf{r}}\nabla U(\mathbf{r})\right]_{r_0} = \begin{bmatrix}U_{xx} & U_{xy} & U_{xz}\\ U_{yx} & U_{yy} & U_{yz}\\ U_{zx} & U_{zy} & U_{zz}\end{bmatrix} \quad (4)$$

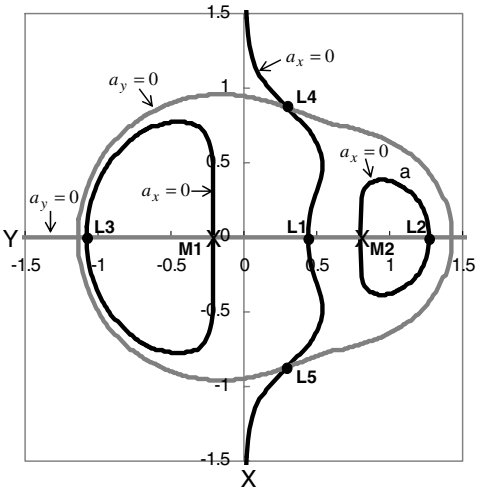

Fig. 3 Superposition of $a_x = 0$ and $a_y = 0$ ($\mu = 0.2$) in the X–Y plane.

Thus, when we set characteristic roots as s and matrices of characteristic equations as $\mathbf{Q}$, the characteristic equation is written in terms of $\det \mathbf{Q}$ as

$$\det \mathbf{Q} = s^6 + (U_{xx} + U_{yy} + U_{zz} + 4)s^4 + \Big(U_{xx}U_{yy} + U_{xx}U_{zz} + U_{yy}U_{zz} - U_{xy}^2 - U_{xz}^2 - U_{yz}^2 + 4U_{zz}\Big)s^2 + U_{xx}U_{yy}U_{zz} + 2U_{xy}U_{xz}U_{yz} - U_{yz}^2U_{xx} - U_{xz}^2U_{yy} - U_{xy}^2U_{zz} \quad (5)$$

The characteristic roots s must satisfy

$$\det \mathbf{Q} = \mathbf{0} \quad (6)$$

Equation (5) can be rewritten by substituting $k = s^2$ as

$$\det \mathbf{Q} = k^3 + (U_{xx} + U_{yy} + U_{zz} + 4)k^2 + \Big(U_{xx}U_{yy} + U_{xx}U_{zz} + U_{yy}U_{zz} - U_{xy}^2 - U_{xz}^2 - U_{yz}^2 + 4U_{zz}\Big)k + U_{xx}U_{yy}U_{zz} + 2U_{xy}U_{xz}U_{yz} - U_{yz}^2U_{xx} - U_{xz}^2U_{yy} - U_{xy}^2U_{zz} \quad (7)$$

A necessary and sufficient condition for an AEP to be linearly stable is that all of the roots are in the left-hand side of the s plane. If there are one or more roots in the right-hand s plane, the system is unstable. Equation (7) is a cubic equation of k. In general, solutions of the cubic equation are either all real numbers or one solution is a real number and the other solutions are imaginary numbers. Noting

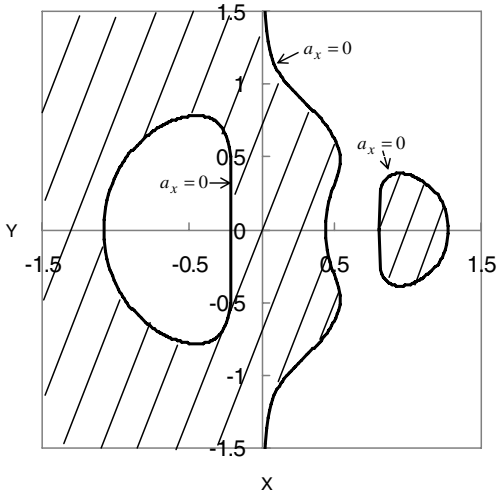

a)

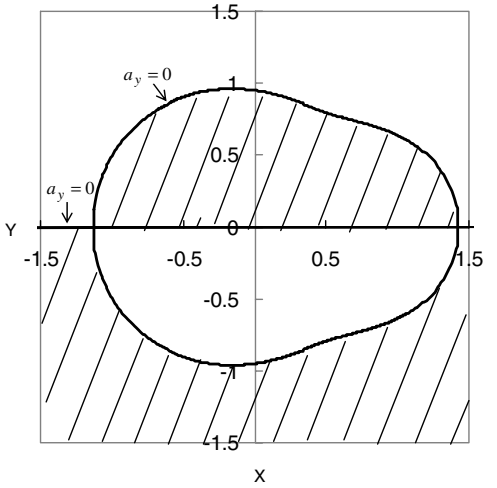

b)

Fig. 2 Plots in the X–Y plane ($\mu = 0.2$) for a) $a_x = 0$ and b) $a_y = 0$; hatched areas show the regions in which a_x (or a_y) is positive.

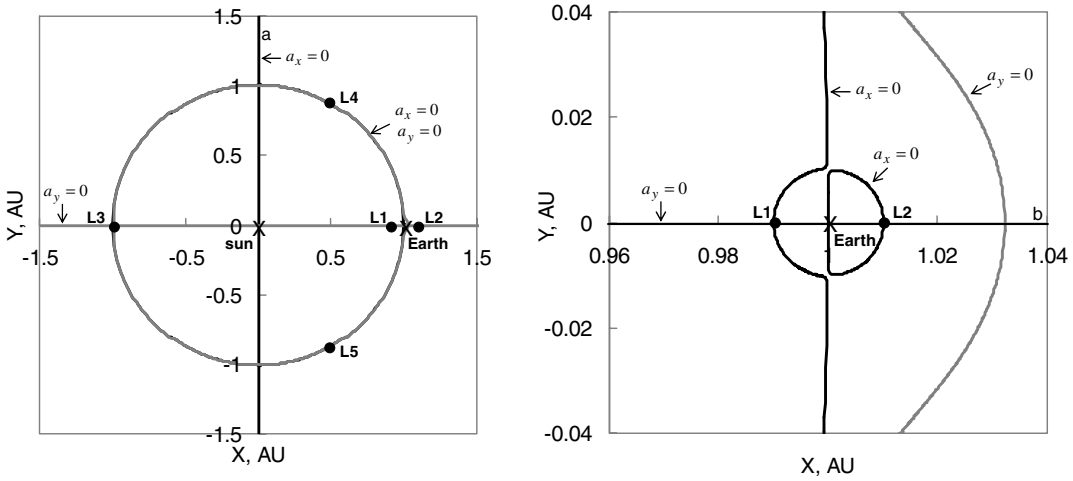

a) Earth–moon system **b) Magnified figure around the Earth (M_2)**

Fig. 4 Superposition of $a_x = 0$ and $a_y = 0$ of the sun–Earth system ($\mu = 3.0404 \times 10^{-6}$) in the X–Y plane.

that $k = s^2$ for all cases, except for those in which all the solutions k of Eq. (7) have real and negative solutions, at least one characteristic root of Eq. (5) exists in the right-hand side of the s plane and the AEP can be regarded as unstable. When all of the solutions k of Eq. (7) are real and negative solutions, all of the characteristic roots s are purely imaginary. Therefore, based on the Hartman–Grobman theorem [14], the AEPs cannot be concluded to be nonlinearly stable even if they are linearly stable. On the other hand, the Kolmogorov–Arnold–Moser (KAM) theory [15] proves that systems with roots only on the imaginary axis can be nonlinearly stable. The KAM theory is valid only for two-degree-of-freedom systems. For three-degree-of-freedom systems, nonlinear stability is not always valid. The orbit discussed in the present Note is three-dimensional, which cannot be covered by the KAM theory. Therefore, we obtain linearly stable AEPs, depending on the conditions of solution k of Eq. (7), and then numerically test the nonlinear stability for some examples.

B. Real and Negative Solutions of the Determinant

Now let us discuss the condition of the real and negative solutions of k. We rewrite Eq. (7) as follows:

$$\det \mathbf{Q} = k^3 + ak^2 + bk + c \tag{8}$$

where the following are shown in [13]

$$\begin{cases} a = U_{xx} + U_{yy} + U_{zz} + 4 = -2 \\ b = U_{xx}U_{yy} + U_{xx}U_{zz} + U_{yy}U_{zz} - U_{xy}^2 - U_{xz}^2 - U_{yz}^2 + 4U_{zz} \\ c = U_{xx}U_{yy}U_{zz} + 2U_{xy}U_{xz}U_{yz} - U_{yz}^2U_{xx} - U_{xz}^2U_{yy} - U_{xy}^2U_{zz} \end{cases} \tag{9}$$

Thus, Eq. (8) is rewritten as

$$\det \mathbf{Q} = k^3 + 2k^2 + bk + c \tag{10}$$

The total number of real and negative solutions of k can be determined by parameters b and c in Eq. (10).

The condition for real solutions is determined from the discriminant of the following cubic equation:

$$k^3 + 2k^2 + bk + c = 0 \tag{11}$$

1. Conditions for Real Solutions

The number of real solutions of k is determined by the discriminant of the cubic equation. (11). The discriminant D of Eq. (11) is then defined as

$$D = \left\{ \left(\frac{q}{2}\right)^2 + \left(\frac{p}{3}\right)^3 \right\} \tag{12}$$

where

$$\begin{cases} p = b - \frac{a^2}{3} = b - \frac{4}{3} \\ q = \frac{16}{27} - \frac{2}{3}b + c \end{cases} \tag{13}$$

When $D \geq 0$, Eq. (11) has three real solutions. When $D < 0$, this equation has only one real solution of k.

2. Conditions for Negative Solutions

The total number of negative solutions of k is obtained by the Descartes sign rule [16]. When the signs of the coefficients of an equation change n times, the equation has n or $n - 2i$ ($i = 1, 2, \ldots$) positive solutions.

Here, the coefficients k^3 and k^2 in Eq. (11) are positive (1 and 2, respectively), and the total number of negative solutions of k is determined only by the signs of coefficients b and c. When the signs of these coefficients do not change (i.e., $b > 0$ and $c > 0$), the number of positive solutions is zero. Then Eq. (11) has either three $D \geq 0$ or one negative solution $D < 0$. In summary, the AEP is stable when $D \geq 0$, $b > 0$, and $c > 0$.

C. Example of Stable Regions

Figures 5–7 show the stable regions (gray areas) satisfying $D \geq 0$, $b > 0$, and $c > 0$ in the X–Y, X–Z, and Y–Z planes, respectively. From these figures, we find that there are linearly stable areas in three-dimensional space. We have numerically tested and confirmed the nonlinear stability for a number of points, one of which is shown in Fig. 8.

IV. Discussion

Here, we discuss the region in which spacecraft can be easily placed in terms of magnitude of acceleration and stability. Figure 9 shows a contour plot of the magnitude of acceleration in the sun–Earth system. The nondimensional magnitude of acceleration $a_0 = 1.0$ corresponds to 5.93×10^{-3} m/s^2 in the sun–Earth system. The boundaries at $D = 0$, $b = 0$, and $c = 0$ are also shown in Fig. 9a, which is equivalent to Fig. 5. The gray area in this figure indicates the stable region. Here, the magnitude of the required acceleration is obtained assuming that other planets such as Mars and Venus are not near the spacecraft with negligible effect. From Fig. 9a, it turns out that the acceleration required for an AEP at $\sim$1.0 AU from the sun is only 10 m/s/year, which corresponds to approximately $a_0 = 5.0 \times 10^{-5}$. In these stable regions, spacecraft can be kept at the AEP with a small control acceleration. Therefore, we can use these AEPs like L4 and L5 points in terms of small control acceleration and stability. From a spacecraft design point of view, telecommand is easier from a spacecraft near the Earth than from one

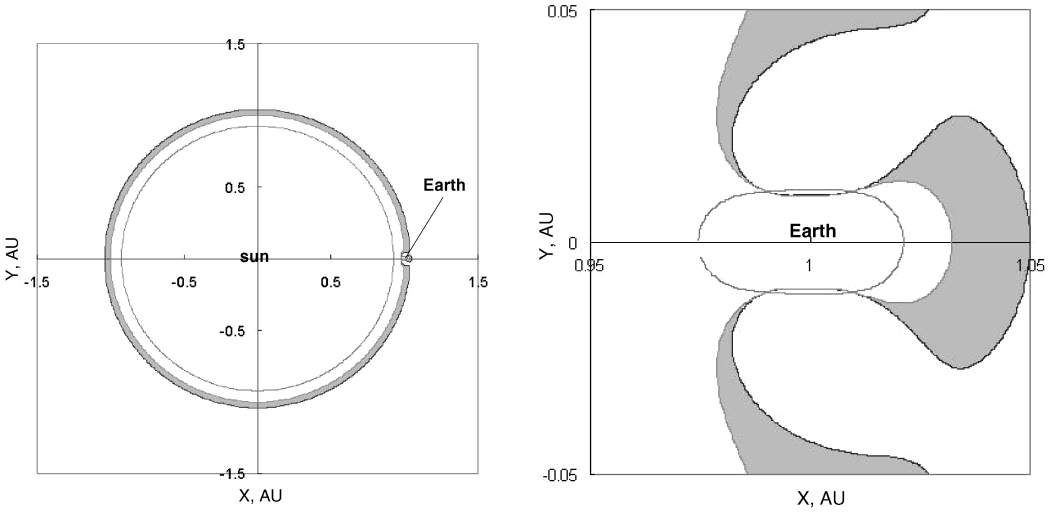

a) Earth–moon system b) Magnified figure around the Earth

Fig. 5 Stable areas (gray) in the *X*–*Y* plane of the sun–Earth system.

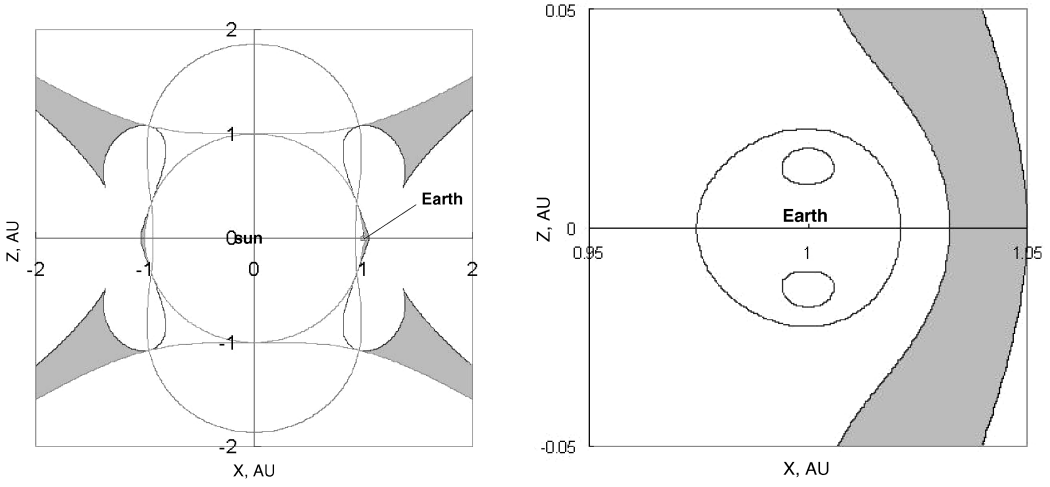

a) Earth–moon system b) Magnified figure around the Earth

Fig. 6 Stable areas (gray) in the *X*–*Z* plane of the sun–Earth system.

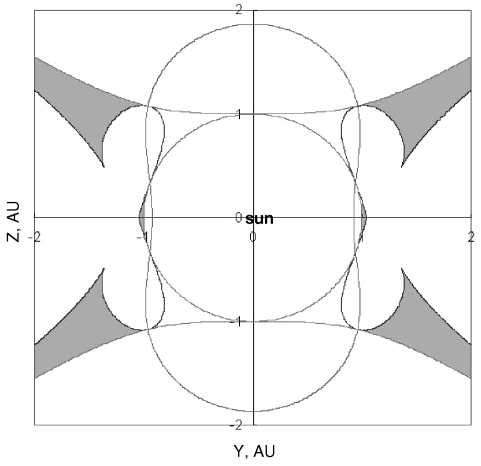

Fig. 7 Stable areas (gray) in the *Y*–*Z* plane of the sun–Earth system, in which the Earth location coincides with that of the sun.

far from the Earth. Therefore, we can choose an AEP nearer to the Earth than the L4 and L5 points, which is very useful for telecommunication. Note that the present Note assumes a restricted three-body problem. In reality, the potential will be very flat for equilibrium at $\sim$1 AU, such that the fourth-body perturbation will become important.

The area in the vicinity of the Earth is also shown in Fig. 9b. The spacecraft can stay at stable areas in the vicinity of the Earth by adding continuous control acceleration $a_0 = 0.03$ (i.e., 17.79×10^{-5} m/s^2).

V. Conclusions

In the present study, we proposed the concept of an artificial equilibrium point (AEP) assisted by continuous control acceleration in the circular restricted three-body problem. AEPs are created by canceling gravitational/centrifugal forces with continuous control acceleration at the nonequilibrium points.

We also discussed the direction and magnitude of required acceleration to turn any arbitrary points into AEPs. The boundaries between positive and negative accelerations in each component are obtained, and the Lagrange points can be derived from the intersections between the boundaries of all acceleration components. From these boundaries, we easily found that there is a region in which the acceleration needed for creating an AEP is very small when the mass ratio is very small, as in the case of the sun–Earth system.

The stability of each AEP was also discussed by linearizing the equations of motion and carrying out a linear stability analysis. The characteristic equations for the equations of motion were transformed into a cubic function. For analyzing stability, we

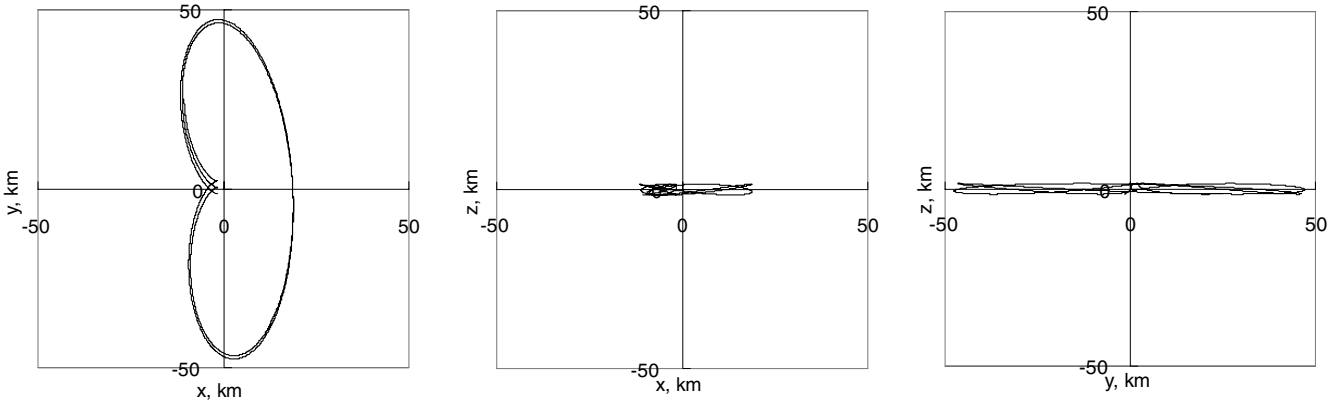

Fig. 8 Numerically integrated motion around the AEP at (1.0, 0.05, 0) AU, in which the centers of the figures correspond to the AEP.

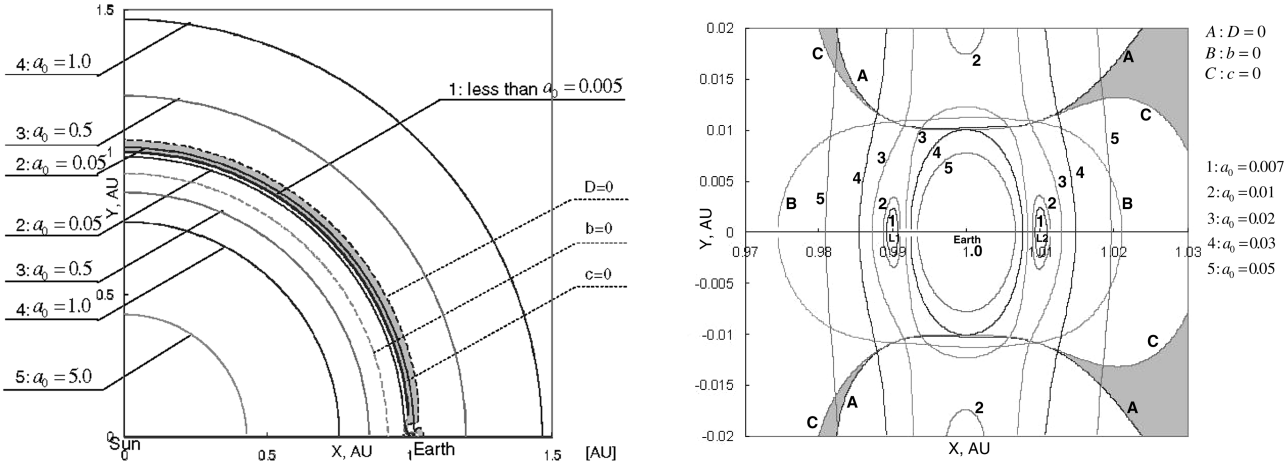

Fig. 9 Contour plots of the magnitude of acceleration ($\mu = 3.0404 \times 10^{-6}$ and $z = 0$): a) 1: less than 2.97×10^{-5}, 2: 2.97×10^{-4} m/s^2, 3: 2.97×10^{-3} m/s^2, 4: 5.93×10^{-3} m/s^2, 5: 2.97×10^{-2} m/s^2; and contour plots of the magnitude of acceleration in the vicinity of the Earth: b) 1: 4.15×10^{-5} m/s^2, 2: 5.93×10^{-4} m/s^2, 3: 1.19×10^{-4} m/s^2, 4: 1.78×10^{-4} m/s^2, 5: 2.97×10^{-4}; gray areas indicate stable regions.

introduced the discriminant of the cubic equation and Descartes sign rule. It turned out that for a small mass-ratio system such as the sun–Earth system, there are stable regions of AEPs with very small control acceleration that are applicable for space missions.

References

[1] Farquhar, R. W., "Lunar Communications with Libration-Point Satellites," *Journal of Spacecraft and Rockets*, Vol. 4, No. 10, 1967, pp. 1383–1384.

[2] Heppenheimer, T. A., "Optimal Controls for Out-of Plane Motion About the Translunar Libration Point," *Journal of Spacecraft and Rockets*, Vol. 17, No. 9, 1970, pp. 1088–1092.

[3] Breakwell, J. V., Kamel, A. A., and Ratner, M. J., "Station-Keeping for a Translunar Communication Station," *Celestial Mechanics*, Vol. 10, No. 3, 1974, pp. 357–373.

[4] Breakwell, J. V., and Brown, J. V., "The 'Halo' Family of 3-Dimensional Periodic Orbits in the Earth–Moon Restricted 3-Body Problem," *Celestial Mechanics*, Vol. 20, Nov. 1979, pp. 389–404.

[5] Wiesel, W., and Shelton, W., "Modal Control of an Unstable Periodic Orbit," *Journal of the Astronautical Sciences*, Vol. 31, No. 1, 1983, pp. 63–76.

[6] Richardson, D. L., "Analytic Construction of Periodic Orbits About the Collinear Points," *Celestial Mechanics*, Vol. 22, Oct. 1980, pp. 241–253.

[7] Simó, C., Gómez, G., Llibre, J., Martínez, R., and Rodriguez, J., "On the Optimal Station Keeping Control of Halo Orbits," *Acta Astronautica*, Vol. 15, Nos. 6/7, 1987, pp. 391–397.

[8] Dusek, H. M., "Motion in the Vicinity of Libration Points of a Generalized Restricted Three-Body Model," *Methods in Astrodynamics and Celestial Mechanics*, Progress in Astronautics and Aeronautics, Vol. 17, 1966, pp. 37–54.

[9] Simmons, J. F. L., McDonald, A. J. C., and Brown, J. C., "The Restricted 3-Body Problem with Radiation Pressure," *Celestial Mechanics*, Vol. 35, Feb. 1985, pp. 145–187.

[10] McInnes, C. R., McDonald, A. J., Simmons, J. F. L., and MacDonald, E., "Solar Sail Parking in Restricted Three-Body Systems," *Journal of Guidance, Control, and Dynamics*, Vol. 17, No. 2, 1994, pp. 399–406.

[11] McInnes, C. R., "Dynamics, Stability and Control of Displaced Non-Keplerian Orbits," *Journal of Guidance, Control, and Dynamics*, Vol. 21, No. 5, 1998, pp. 799–805.

[12] Broschart, S. B., and Scheeres, D. J., "Control of Hovering Spacecraft Near Small Bodies: Application to Asteroid 25143 Itokawa," *Journal of Guidance, Control, and Dynamics*, Vol. 28, No. 2, 2005, pp. 343–354.

[13] Morimoto, M., Yamakawa, H., and Uesugi, K., "Periodic Orbits with Low-Thrust Propulsion in the Restricted Three-Body Problem," *Journal of Guidance, Control, and Dynamics*, Vol. 29, No. 5, 2006, pp. 1131–1139.

[14] Robinson, C., *Dynamical Systems: Stability, Symbolic Dynamics, and Chaos*, 2nd ed., CRC Press, Boca Raton, FL, 1999, Chap. 5.

[15] Boccaletti, D., and Pucacco, G., "Perturbative and Geometrical Methods," *Theory of Orbits*, Vol. 2, Springer–Verlag, Berlin, 1999, pp. 99–106.

[16] Henrici, P., "Power Series, Integration, Conformal Mapping, Location of Zeros," *Applied and Computational Complex Analysis*, Vol. 1, Wiley, New York, 1988, pp. 439–443.